Smart User Interface for Mobile Consumer Devices Using Model-Based Eye-Gaze Estimation

Nadeem Iqbal, Hwaran Lee and Soo-Young Lee, *Member*, IEEE

Abstract—*A smart user-interface for mobile consumer devices was developed using a robust eye-gaze system without any hand motion. Using one camera and one display already available in popular mobile devices, the eye-gaze system estimates the visual angle, which shows the area of interest on the display to indicate the position of the cursor. Three novel techniques were developed to make the system robust, user-independent, and head/device motion invariant. First, by carefully investigating the geometric relation between the device and the user's cornea, a new algorithm was developed to estimate the cornea center position, which is directly related to the optical axis of the eye. Unlike previous algorithms, it does not utilize the user-dependent cornea radius. Second, to make the system robust for practical application, an algorithm was developed to compensate for imaging position errors due to the finite camera resolution. Third, a binocular algorithm was developed to estimate the user-dependent angular offsets between the optical and visual axes with only single point calibration. The proposed system was demonstrated to be accurate enough for many practical mobile user interfaces..*[1]

Index Terms—Human-computer interface, multimodal user interface, model-based eye-gaze estimation, binocular gaze relation.

I. Introduction

Smart mobile devices require a better human-machine interface. Many technologies have been developed recently for multimodal human-machine interfaces including eye-gaze tracking systems [1-4]. A new game system had been reported with an integrated user-interface consisting of a head-mounted display, an eye-gaze tracking system, a gesture recognizer, and a bio-signal classifier [1-2]. An eye-gaze tracking system and an electroencephalogram (EEG) classifier had also been integrated for a new computer interface [3]. Particularly for handheld devices where one hand is pre-occupied, an eye-gaze-based interface would be quite advantageous to free the other hand for other operations. The cursor could be moved naturally by the eye gaze, and the equivalent of mouse clicks or screen touches could be implemented by eye blinking, prolonged gaze fixation, or a simple device shaking motion. Furthermore, increased processing power and high-resolution cameras can now make the eye-gaze tracking affordable for the new generation of mobile devices.

Eye-gaze tracking technologies are categorized into two approaches, two-dimensional (2D) interpolation (or regression) and three-dimensional (3D) model-based (or geometric) methods [5]. The 2D interpolation methods use a mapping function from 2D eye-image features (or raw images) to determine the gaze position [6]. Although the interpolation methods are quite simple, they have fundamental problems with head movement and therefore are not suitable for mobile devices. The 3D model-based approaches utilize the 3D geometric relationship among the eye(s), camera, and display [7-17]. The optical axis is estimated as the line between the cornea center and the pupil center, and the visual axis is obtained from the optical axis with user-dependent offset angles. The model-based approaches are capable of handling relative motion between the device and the user's eye, and therefore have potential advantage for mobile applications. Although multiple cameras are advantageous [7], eye-gaze systems for popular mobile devices with only one camera are considered here.

In order to estimate the visual axis accurately, it is necessary to know a few user-dependent parameters such as cornea radius and offset angles between the optical and visual axes. The visual axis is sensitive to these user parameters, of which accurate estimation has required bulky head-fixed or head-mounted systems. It is still challenging to obtain accurate eye-gaze estimation for mobile consumer devices with one camera and a small display screen while allowing head motion [18-19].

In this paper, a new mobile device is presented with multi-modal user interfaces, where the eye-gaze estimation plays an important role of cursor positioning in a natural manner. A new algorithm is proposed for estimating cornea center and cornea radius simultaneously via a single camera, and therefore it is not necessary to know the user-dependent cornea radius in advance. A method has been devised to reduce error due to finite pixel sizes of the camera. Furthermore, the user-dependent angle parameters between the optical and visual axes are obtained through a binocular gaze algorithm.

The remainder of this paper is organized as follows: Section II presents the cornea center estimation algorithm, Section III describes error correction methods, Section IV discusses the binocular-gaze algorithm, and the experimental setup and results are presented in Section V.

[1] This work was supported by the Basic Science Research Program of the National Research Foundation of Korea (NRF), funded by the Ministry of Education, Science and Technology (2009-0092812, 2010-0028722, and 2011-0029816).

N. Iqbal is with the Department of Bio and Brian Engineering, Korea Advanced Institute of Science and Technology (KAIST), Daejeon, 305-701 Republic of Korea. (e-mail: nadeem@neuron.kaist.ac.kr).

H. Lee is with the Brain Science Research Center, KAIST, Daejeon, 305-701, Republic of Korea.(e-mail: leehr90@kaist.ac.kr).

S.Y. Lee is with the Department of Electrical Engineering and Brain Science Research Center, KAIST, Daejeon, 305-701 Republic of Korea. (e-mail: sylee@kaist.ac.kr).

Contributed Paper
Manuscript received 10/15/12
Current version published 03/25/13
Electronic version published 03/25/13.

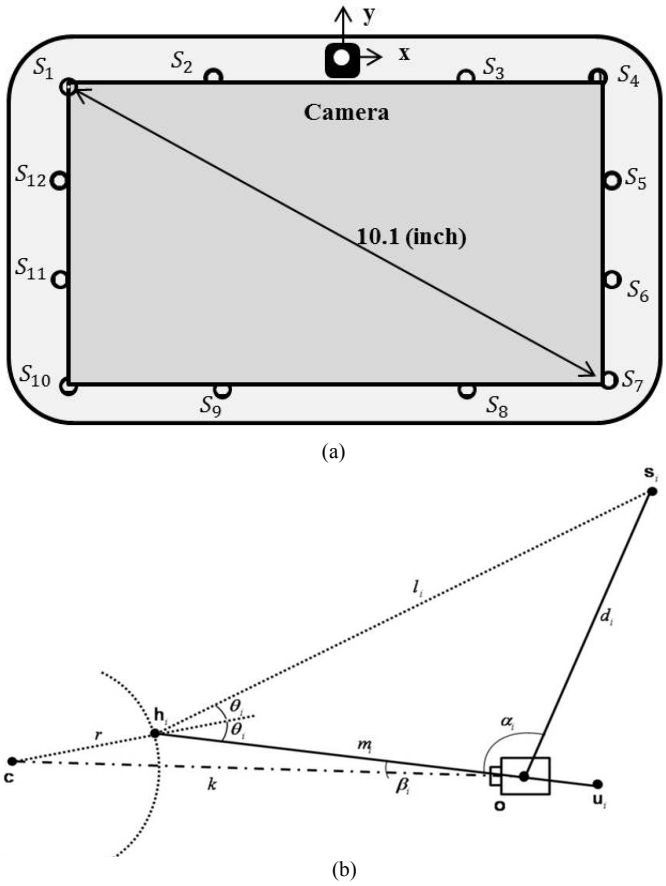

Fig. 1. (a) A mobile device with eye-gaze estimation system consisting of a camera and several light sources for glint generation. (b) Geometrical optical relation among a light source, camera, and cornea.

II. Cornea Center and Radius Estimation

The optical axis is defined as the line between the cornea center and pupil center. The cornea is a protective transparent membrane on the surface of the eye [20]. The cornea radius is a subject-dependent parameter which had been used for the estimation of the cornea center. Therefore, an accurate estimation of the cornea radius in advance was very important.

There are two approaches for finding the cornea radius: the calibration- and non-calibration-based approaches. The calibration-based approach determines the cornea radius through a calibration procedure in which the subject fixates on several points presented sequentially on the display screen [17]. The non-calibration approach used multiple cameras to estimate the cornea center [18]. Using multiple cameras reduces the subject-dependent parameter but increases the system complexity. By carefully investigating the geometrical relation among cornea and devices, a new algorithm is now presented to estimate the cornea center and cornea radius simultaneously without any calibration.

As shown in Figure 1(a), let's consider a mobile device with a camera and several light sources for glint generation. In Figure 1(b), the geometric relation between the light source **s**, camera center **o**, and cornea center **c** is shown where all points are represented in bold font as 3D vectors of a world coordinate system. Here the camera center **o** is assumed to be the center of the world coordinate system for simplicity. The cornea of the eye is assumed to be a spherical surface with the cornea center **c** and radius r. In order to analyze the image formation process, we consider the i-th incident ray to come from the light source $\mathbf{s}_i$ and hit the cornea surface at the incidence point $\mathbf{h}_i$. The reflected ray passes through the camera center and hits the image plane at glint point $\mathbf{u}_i$. The camera center, cornea center, and light source are coplanar, and according to the law of reflection, the angle of incidence θ_i is equal to the angle of reflection.

From trigonometric rules, the relation between the cornea radius r and the distance between the cornea center and the camera center k is derived as

$$\frac{k_i}{r_i} = \frac{\sin\theta_i}{\sin\beta_i} \tag{1}$$

$$\frac{r_i}{d_i} = \frac{\sin\beta_i}{\sin(\theta_i - \beta_i)} \frac{\sin(2\theta_i + \alpha_i)}{\sin 2\theta_i} \tag{2}$$

where the subscript "i" represents the i-th light source location, d is the distance between the light source and the camera center, α is the angle between the light source and the glint vector, and θ_i is the reflection angle.

Each light source defines a plane with three positions, **o**, $\mathbf{s}_i$, and $\mathbf{u}_i$, with **c** required to be located in the plane. Two planes defined from two light sources intersect along a line on which both **o** and **c** are located. We defined $\mathbf{w}_{ij}$ as the unit vector in the direction of the intersection line of the planes of two light sources, $\mathbf{s}_i$ and $\mathbf{s}_j$, and calculate it using vector multiplication as

$$\hat{\mathbf{w}}_{ij} = (\mathbf{s}_i \times \mathbf{u}_i) \times (\mathbf{s}_j \times \mathbf{u}_j), \mathbf{w}_{ij} = \frac{\hat{\mathbf{w}}_{ij}}{\|\hat{\mathbf{w}}_{ij}\|} \tag{3}$$

Since **c** and $\mathbf{w}_{ij}$ are in the same (or the opposite) direction, the angle β_i is uniquely determined from two light sources. Equation (2) shows that θ_i is depends only on r, and from (1) k/r becomes a function of r only. Since r and k should be the same for all light sources, the optimum estimation of r can be obtained by minimizing the following cost function:

$$f(r) = \frac{1}{2}\sum_{i=1}^{L}\sum_{j>i}^{L}\left(\frac{\sin\theta_i(r)}{\sin\beta_i} - \frac{\sin\theta_j(r)}{\sin\beta_j}\right)^2 \tag{4}$$

where θ_i is defined as a function of r for d_i, α_i, and β_i from (2). It is important to notice that, unlike previous formulations, only one variable, r, is used to optimize the function, and the simple gradient descent iteration is applied as

$$r = r - \eta\frac{df(r)}{dr}, \tag{5}$$

where η is the learning rate. The derivative of the cost function with respect to r is obtained as

$$\frac{df}{dr} = \sum_{i=1}^{L}\sum_{j>i}^{L}\left(\begin{array}{l}\left(\frac{\sin\theta_i}{\sin\beta_i} - \frac{\sin\theta_j}{\sin\beta_j}\right)\cdot \\ \left(\frac{\cos\theta_i}{\sin\beta_i}\frac{d\theta_i}{dr} - \frac{\cos\theta_j}{\sin\beta_j}\frac{d\theta_i}{dr}\right)\end{array}\right) \tag{6}$$

with

$$\frac{d\theta_i}{dr} = 1 \Big/ \frac{dr}{d\theta_i} \quad .$$

Here the uniqueness of the inverse function $\theta_i(r)$ in (6) is obtained because of the monotonic relationship between r and θ_i in (2) within the parameter range of interest, i.e., $0 < \theta_i < \pi/4$. At each iteration, new θ_i values are estimated by numerically solving the nonlinear equation (2) for new r values. It has been observed that after a few iterations of (5), the cost function converges to a minimum. Then, from (1), the value of k and the cornea center position $\mathbf{c}$ are obtained.

The proposed method requires an initial value for the cornea radius. The cornea radius is defined as the angle of reflection in (2). Therefore, the reflection angle is expressed as a function of the distance between the incidence point and the camera center m as follows:

$$\theta_i = \frac{1}{2}\arcsin\left(\frac{d_i \sin\alpha_i}{\left(d_i^2 + m_i^2 - 2d_i m_i \cos\alpha_i\right)^{\frac{1}{2}}}\right) \tag{7}$$

In the experimental study, the distance between the incidence point and the camera center was similar to the distance between the subject's eye and the camera center. Therefore, the average distance between the subject and the mobile device was used to find the initial reflection angle corresponding to each light source. In contrast, the previous algorithms required initial values for both the cornea center $\mathbf{c}$ and the cornea radius r.

III. Error Correction for Glint Position

The proposed algorithm for estimating a cornea radius is sensitive to errors on glint image position $\mathbf{u}_i$. The camera position is estimated through the camera calibration procedure or from the manufacture's specifications. However, slight changes in the accuracy of the image position $\mathbf{u}_i$ result in large errors in the estimated cornea radius r and cornea center $\mathbf{c}$, and therefore gaze positions. Therefore, a method has been devised to reduce the error at the glint image position.

For a system with L light sources, all values of $\mathbf{w}_{ij}$ from different (i,j) combinations should be identical. However, because of error on $\mathbf{u}_i$, they become different. To reduce this error, we used the average cornea $\mathbf{w}_{av}$, which is defined as

$$\hat{\mathbf{w}}_{av} = \frac{2}{L(L-1)}\sum_{i=1}^{L}\sum_{j>i}^{L}\mathbf{w}_{ij}, \quad \mathbf{w}_{av} = \frac{\hat{\mathbf{w}}_{av}}{\left\|\hat{\mathbf{w}}_{av}\right\|} \tag{8}$$

However, because of this error correction, the camera imaging position is no longer on the $\boldsymbol{P}_i$ plane defined by $\mathbf{c}$, $\mathbf{s}_i$, and $\mathbf{o}$. Therefore, we propose to project $\mathbf{u}_i$ on the $\boldsymbol{P}_i$ plane for error reduction. Since the normal vector $\mathbf{n}_i$ to this plane is defined as

$$\mathbf{n}_i = \mathbf{w}_{av} \times \mathbf{s}_i \tag{9}$$

the projection-corrected position $\mathbf{u}_i^c$ is obtained as

$$\mathbf{u}_i^c = \mathbf{u}_i - (\mathbf{u}_i \cdot \mathbf{n}_i)\mathbf{n}_i \tag{10}$$

and used for cornea radius estimation.

Light source location is analyzed and selected in order to improve the estimation precision. In (4), the locations of the two light sources are selected such that the angles (namely, β_i and β_j) are unequal. This inequality implies that the large difference in distance between the two light sources from the camera center is required for the better convergence. However, if the angles are equal, the difference in distance between the two light sources from the camera center is small. The objective function then prevents the convergence to an optimum solution. Therefore, light source pairs were selected to result in large differences of β_i.

IV. Binocular Gaze Estimation

In order to determine point of gaze (POG), the visual axis direction is required. The visual axis of the eye is defined between the cornea center and the fovea. The fovea is a small area with a diameter of about 1.2° in the retina. During gazing, the eye is oriented in such a way that the observed object projects itself on the fovea. It is known that the actual visual axis is not the same as the optical axis defined between the cornea and the pupil centers [16]. The offset between the optical and visual axes is compensated for with single point calibration.

The distance between the pupil and the cornea centers is expressed as

$$\left\|\mathbf{p} - \mathbf{c}\right\| = k_p \tag{11}$$

where $\mathbf{p}$ is the pupil center and $\mathbf{c}$ is cornea center. The 3D pupil center is reconstructed by defining a pupil ray that comes out from the cornea surface, passes through the camera center $\mathbf{o}$, and hits the image plane at the image point $\mathbf{v}_\mathrm{p}$. The pupil ray, having a direction vector $\mathbf{b}$, is written in parametric form as $\mathbf{p} = \delta_\mathrm{p}\mathbf{b}$ for some scalar δ_p. We express $\mathbf{p}$ as a function of the distance parameter k_p as

$$\mathbf{p} = \left(k\left(\mathbf{b}^\mathrm{T}\mathbf{w}\right) - \sqrt{\left(k(\mathbf{b}^\mathrm{T}\mathbf{w})\right)^2 + k_p^2 - k^2}\right)\mathbf{b} \tag{12}$$

The cornea center $\mathbf{c}$ and the direction vector $\mathbf{b}$ are assumed to be known. The parameter k_p is subject-dependent and is estimated using a binocular gaze algorithm. Having calculated the pupil center and knowing the cornea center, we determine the optical axis, and the normalized optical axis is converted to spherical coordinates:

$$\phi = \arcsin\frac{\mathbf{p_y} - \mathbf{c_y}}{k_p}, \quad \psi = -\arctan\frac{\mathbf{p_x} - \mathbf{c_x}}{\mathbf{p_z} - \mathbf{c_z}} \tag{13}$$

where ϕ is a vertical angle and ψ is a horizontal angle. Here, the spherical coordinate system used. The visual axis is defined as having a vertical angle $(\phi + \varphi)$ and a horizontal angle $(\psi + \gamma)$. The two angles φ and γ are subject-dependent and need to be estimated through calibration. The POG intersects with the display screen, and since the geometric information of the screen is available, the POG is defined as

$$\mathbf{g}_x = \mathbf{c}_x + \mathbf{c}_z\tan(\psi + \gamma), \quad \mathbf{g}_y = \mathbf{c}_y + \mathbf{c}_z\frac{\tan(\phi + \varphi),}{\cos(\psi + \gamma)} \tag{14}$$

Solving the above system of equations for the binocular POG requires four angle parameters with two angles for each visual axis and distance parameter. In this case, we have more scalar unknowns than equations, and need more than one point for calibration or increase the system complexity by using two cameras instead of one. In order to use single point calibration with a single camera, we introduced the binocular eye algorithm to estimate the unknown parameters here.

During eye gazing, both eyes are oriented in such a way that their visual axes converge to the same position. This implies that the horizontal and vertical angles between the optical and visual axes of both eyes are equal. Anatomically, it is evident that the human body is symmetric around the sagittal plane. We also assumed that the distance between the cornea center and the pupil center is identical in both eyes. Therefore, the above assumptions are expressed as

$$\begin{aligned} \varphi &= \varphi_L = \varphi_R \\ \gamma &= \gamma_L = \gamma_R \\ k_p &= k_p^L = k_p^R \end{aligned} \tag{15}$$

where the subscript "*L*" indicates the left eye and "*R*" indicates the right eye. The subject-dependent parameter for binocular eye relation with the above assumption reduces to three subject parameters: the angle parameters (φ and γ) and the distance parameter (k_p). In order to optimize these unknown parameters for binocular vision, we devised the following objective function

$$f\left(\varphi,\gamma,k_p\right) = \left\|\mathbf{g}_L - \mathbf{g}\right\|^2 + \left\|\mathbf{g}_R - \mathbf{g}\right\|^2 \tag{16}$$

where $\mathbf{g}_L$ is the left POG and $\mathbf{g}_R$ is the right POG. The calibration point is $\mathbf{g}$. The objective function is non-linear. The Levenberg-Marquardt [21] algorithm was used to find the optimum values for the unknown parameters. The above algorithm reconstructs the visual axis and estimates the POG with a simple configuration of a single camera

V. Experimental Results

In order to validate the performance of the proposed algorithms, we used multiple light sources attached to a handheld device as shown in Figure 1(a). A 2-megapixel video camera at 30 fps is centered at the top of the screen. The distance between the subject and the handheld device is about 200 mm. The user's head is moving around in front of the mobile device. The system parameters, namely, the positions of light sources and the camera focal length, must be estimated once in the initial design phase or obtained from the manufacture's specifications. In this study, we performed three experiments to analyze the performance of the algorithm for user-dependent parameters.

In the first experiment, we observed the performance of our algorithm for finding the cornea radius and cornea center, and compared this with existing algorithms [18]. A pair of light sources attached to the display screen is used in order to estimate the cornea radius by iteratively minimizing (4) with different initial distances between the camera center and the user's eye. Then, the reflection angle θ_i and cornea center $\mathbf{c}$ are calculated from (2) and (1), respectively. The existing algorithm using the same experimental setup required both the initial cornea center and the cornea radius.

TABLE I
Estimated Cornea radius with Proposed and Existing Method

	Initial Distance k			
	190 mm	**195 mm**	**205 mm**	**210 mm**
Existing method				
r-init = 8.97	8.91	7.67	7.70	8.90
r-init = 7.02	7.31	7.79	7.78	7.58
r-init by (7)	7.32	7.80	7.79	8.36
Proposed				
r-init by(7)	**7.80**	**7.80**	**7.80**	**7.80**

TABLE II
Error Correction Performance

Glint Image Error Level	Eye-Gaze Angular error (°)		
	Without-correction	**With correction**	**With 5-frame average and correction**
0.1 PIXEL	1.14°±0.99°	0.92°±0.75°	0.20°±0.19°
0.2 PIXEL	2.02°±1.92°	1.45°±1.39°	0.60°±0.48°
0.3 PIXEL	2.99°±2.05°	2.32°±1.98°	0.98°±0.59°
0.4 PIXEL	4.11°±2.99°	3.01°±2.42°	1.16°±0.89°
0.5 PIXEL	5.08°±4.12°	3.70°±3.21°	1.30°±1.01°

As shown in Table I, two initial cornea radius values, 15% larger (8.97 mm) and 10% smaller (7.02 mm) than the actual value, were used as the initial value, *r*-init, for the existing method. Furthermore, the initial cornea radius was estimated from (7) and used for both the proposed and existing methods. The proposed algorithm estimated the true cornea radius at 7.8 mm for all different distances. Therefore, the proposed cornea estimation method does not depend on the distance. This implies that the proposed algorithm allows the subject to move during the eye-gaze estimation. As can be observed in Table I, for each initial distance and for every initial cornea radius, the results of the existing method vary. However, this slight variation leads to a large angular error for eye-gaze estimation.

Next, the performance of the glint image error correction algorithm was tested. One hundred independent realizations of an additive zero-mean Gaussian noise with standard deviations between 0.1 and 0.5 pixels were added to the image position in order to simulate the error in $\mathbf{u}_i$. The angular errors between the true and estimated optical axes are estimated. The estimated optical axis was obtained from the estimated cornea and pupil center positions. The cornea radius and cornea centers were estimated using the proposed algorithm in Section II. For a system with *L* light sources, we obtained the average cornea vector $\mathbf{w}_{av}$ as (8), and corrected glint image position $\mathbf{u}_i$ by (10). The average and standard deviation of the angular errors are summarized in Table II for the 100 random realizations. The results in Table II show that the proposed error correction method reduced the angular error by 20%. To reduce the error further, we also applied the frame average of

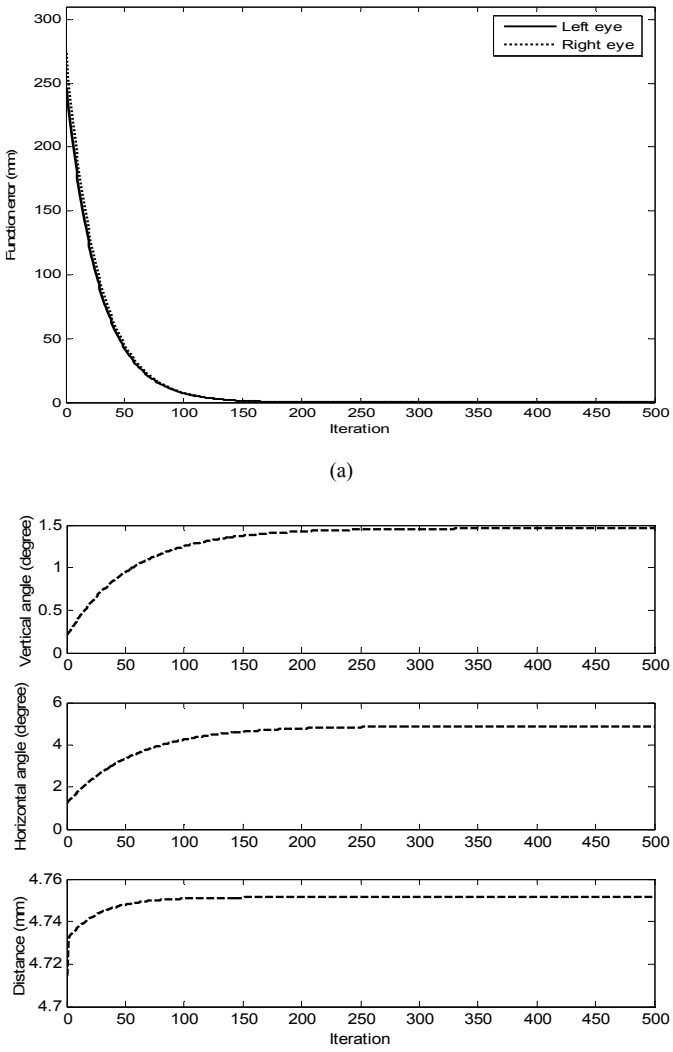

Fig. 2. Convergence of the user-dependent parameters with binocular gaze estimation. (a) Error between left and right POGs, and (b) user-dependent parameters.

$\mathbf{u}_i$ for five frames in each experiment. By averaging five frames, i.e., about 0.16 s at the frame rate of 30 fps, the angular errors become 0.98° and 1.30° with 0.3 and 0.5 pixel errors, respectively. Many commercial eye-gaze systems with bulky hardware offer about 1° angular error. However, the distance between eye and display screen is much smaller for mobile devices than that of the bulky commercial systems, and the above 0.98° and 1.30° errors may be acceptable.

In the third experiment, to measure the user-specific parameters, i.e. k_p, φ, and γ, the proposed binocular one-point calibration procedure was performed. During the calibration procedure, the subject was asked to fix their gaze on one point on the display screen. Then, the user parameters were obtained by minimizing (16). As shown in Figure 2(a), the left and the right POGs effectively converge to the same calibrated point on the screen. In Figure 2(b), after 500 iterations the solution converges to the true user-dependent parameter values. Since the calculation is simple, this iteration was done in real time.

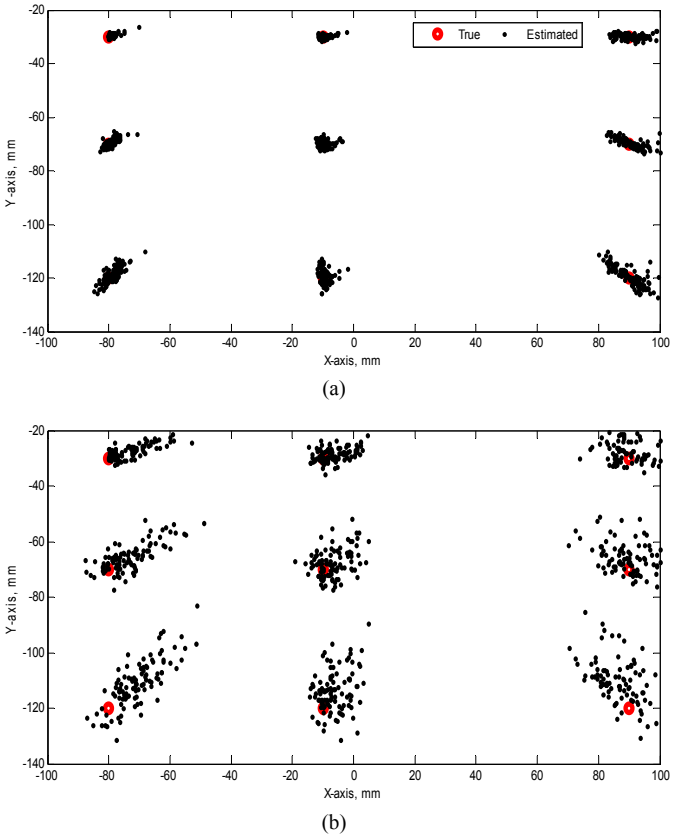

Fig. 3. Eye gaze estimation with a smart handheld device. (a) 0.1 pixel errors for both glint and pupil center positions with 5-frame average, and (b) 0.3 pixel errors for both glint and pupil center positions with 5-frame average.

TABLE III
ANGULAR GAZE ERROR WITH 5-FRAME AVERAGE AT DIFFERENT GAZE POSITIONS

	0.1 pixel error on both glint and pupil center		
	Left Column	Center Column	Right Column
Top Row	0.30°	0.33°	0.97°
Middle Row	0.54°	0.47°	1.06°
Bottom Row	0.97°	0.43°	1.41°

	0.3 pixel error on both glint and pupil center		
	Left Column	Center Column	Right Column
Top Row	1.83°	1.35°	2.27°
Middle Row	2.52°	1.75°	2.49°
Bottom Row	3.89°	2.52°	3.63°

Using the optimized parameter values, the POG estimation was performed for nine fixation points on the display screen. Also, Gaussian noise was added to both the glint image and pupil image positions with 0.1 and 0.3 pixels each. The estimated point-of-gaze positions of 100 realizations were shown in the Figure 3. Also, the average angular errors are summarized in Table III. These results show that the accuracy of the eye-gaze positions and angular errors is somewhat worse than that of the commercial bulky systems. However, it may still be good enough to identify which part of the display screen users are looking at for many simple menu-driven user

interfaces. For systems requiring higher accuracy the averaging may be done with more frames. Actually the averaging with 10-frames still provides 300 ms and 150 ms temporal resolution with 30 and 60 frames per seconds frame rates, respectively, which are good enough for real-time applications.

VI. Conclusion

The proposed user interface for hand-held mobile devices in this paper is based on 3D geometrical model-based eye–gaze estimation. The eye-gaze provides the point-of-interest on the display screen, which may naturally be used to control the cursor. The push button need be implemented by a prolonged gaze fixation, or another modality such as acceleration and EEG. This system is non-intrusive and allows users to move head and hands freely. It has a wide range of application and great potential for use with mobile consumer devices.

Compared to existing methods, the developed system is simple and robust on imaging position errors of glint and pupil center. This advantage comes from new careful investigation of geometrical relation among handheld device and user eyes.

The proposed system is accurate enough for applications requiring moderate accuracy of the cursor control. In the future the emergence of better camera and display will provide much better gazing accuracy for nearly every application on mobile consumer devices.

Acknowledgment

The author expresses their gratitude to Wonil Chang and Choong Hwan Choi for valuable discussion. The author would also like to appreciate Professor Arantxa Villanueva for providing the pseudo-code of her algorithm for comparison.

References

[1] H. Heo, E.C. Lee, K.R. Park, C.J. Kim, and M. Whang, "A realistic game system using multi-modal user interfaces," *IEEE Trans. Consumer Electron.,* vol. 56, no. 3, pp. 1364-1372, Aug. 2010.

[2] P.M. Corcoran, F. Nanu, S. Petrescu, and P. Bigioi, "Real-Time eye gaze tracking for gaming design and consumer electronics systems," *IEEE Trans. Consumer Electron.,* vol. 58, no. 2, pp. 347-355, May. 2012.

[3] J.W. Bang, E.C. Lee, and K.R. Park, "New computer interface combining gaze tracking and brainwave measurements," *IEEE Trans. Consumer Electron.,* vol. 57, no. 4, pp. 1646-1651, Nov. 2011.

[4] H.C. Lee, D.T. Luong, C.W. Cho, E.C. Lee, and K.R. Park, "Gaze tracking system at a distance for controlling IPTV," *IEEE Trans. Consumer Electron.,* vol. 56, no. 4, pp. 2577-2583, Nov. 2010.

[5] D.W. Hansen, and Q. Ji, "In the eye of the beholder: A survey of models for eyes and gaze," *IEEE Trans. Pattern Anal. Mach. Intell.*, vol. 32, no. 3, pp. 478-500, 2010.

[6] C.H. Morimoto, and M.R.M. Mimica, "Eye gaze tracking techniques for interactive applications," *Comput. Vision Image Understanding.,* vol. 98, no. 1, pp. 4-24, Apr. 2005.

[7] T. Nagamatsu, R. Sugano, Y. Iwamoto, J. Kamahara and N. Tanaka, "User-calibration-free gaze estimation method using a binocular 3D eye model," *IEICE Trans. Inf. Syst.*, vol. E94-D, no.9, pp.1817-1829, Sept. 2011.

[8] D. Model and M. Eizenman, "User-calibration-free remote gaze estimation system," *Proc. 2010 Symp. Eye-Tracking Res. and Appl.*, pp.29-36, Mar. 2010.

[9] D. H. Yoo and M. J. Chung, "A novel non-intrusive eye gaze estimation using cross-ratio under large head motion," *Comput. Vision Image Understanding*, vol. 98, no. 1, pp. 25-51, Apr. 2005.

[10] J.G. Wang, E. Sung, and R. Venkateswarlu, "Estimating the eye gaze from one eye," *Comput. Vision Image Understanding.*, vol. 98, no. 1, pp. 83-103, Apr., 2005.

[11] E.D. Guestrin and M. Eizenman, "Remote point-of-gaze estimation requiring a single-point calibration for application with infants," *ETRA2008 Proc. Eye Tracking Res. Appl. Symp*., pp. 267-274, Mar. 2008.

[12] A. Villanueva, R. Cabeza, and S. Porta, "Eye tracking: pupil orientation geometrical modeling," *Image and Vision Comput.*, vol. 24, no. 7, pp. 663-679, Jul. 2006.

[13] A. Villanueva, R. Cabeza, and S. Porta, "Gaze tracking system model based on physical parameter," *Int. J. Pattern Recognit. Artif. Intell.*, vol. 21, no. 5, pp. 855-977, 2007.

[14] K.P. White Jr., T.E. Hutchinson, and J.M. Carley, "Spatially dynamic calibration of an eye-tracking system," *IEEE Trans. Syst., Man, and Cybern.*, vol. 23, no. 4, pp. 1162-1168, July/Aug. 1993.

[15] B. Noureddin, P.D. Lawrence, and C.F. Man, "A non-contact device for tracking gaze in a human computer interface," *Comput. Vision and Image Understanding*, vol. 98, no. 1, pp. 52-82, 2005.

[16] S.W. Shih and J. Liu, "A novel approach to 3D gaze tracking using stereo cameras," *IEEE Trans. Syst., Man, and Cybern.*, Part B: Cybern., vol. 34, no. 1, pp. 234-245, Feb. 2004.

[17] E.D. Guestrin and M. Eizenman, "General theory of remote gaze estimation using the pupil center and corneal reflections," *IEEE Trans. Biomed., Eng*., vol. 53, no. 6, pp. 1124-1133, June 2006.

[18] A. Villanueva, and R. Cabeza, "A novel gaze estimation system calibration point," *IEEE Trans. Syst., Man, and Cybern*., vol. 38, no. 4, pp. 1123-1138, Aug. 2008.

[19] J. Sun, C. Yang, J. Liu, and X. Yang, "Gaze tracking based on similarity between spatial triangles and two stage calibration," *Electron. Lett.*, vol. 47, no. 4, pp.254-255, Feb. 2011.

[20] R. Carpenter, *Movement of the Eyes*, Pion Limited: London, 1988,

[21] R. Hartley and A. Zisserman, *Multiple view geometry in computer vision*, Cambridge University Press: London, 2003, pp. 600-602

Biographies

Nadeem Iqbal received a Master degree in computer system engineering from the GIK Institute, Topi, Pakistan, in 2003. He is a PhD student in Bio and Brian engineering from KAIST, Daejeon, Republic of Korea. His research interests include image processing, eye gaze tracking, image-based eye analysis, supervised and unsupervised machine learning methods and computer vision.

Hawarn Lee is currently an undergraduate student in the Mathematical Science at the Korea Advanced Institute of Science and Technology (KAIST), Deajeon, Republic of Korea. Her research interests include computational neuroscience, machine learning, and HCI

Soo-Young Lee (M'83) received B.S. degree from Seoul National University, Seoul, Korea, in 1975, M.S. degree from the Korea Advanced Institute of Science and Technology (KAIST), Daejeon, Korea, in 1977, and Ph.D. degree from the Polytechnic Institute of New York, Brooklyn, in 1984. He was with Taihan Engineering Company, Seoul, from 1977 to 1980. He was with the General Physics Corporation, Columbia, MD, from 1982 to 1985. In 1986, he joined the Department of Electrical Engineering, KAIST, as an Assistant Professor, and now is a Full Professor in the same department and also in the Department of Bio and Brain Engineering. From 1998 he serves as Director of Brain Science Research Center at KAIST, and had led a big national research program on Neuroinformatics. His current research interests include artificial brains, human-like intelligent systems/robots based on biological information processing mechanisms in brains, mathematical models, neuromorphic chips, real-world applications, intelligent man-machine interfaces with electroencephalograms, and eye gaze.